Multi-Fiber, MT Ferrule Endface Fiber Tip Displacement Model for Physical Contact Interconnects

Michael Gurreri, James Kevern, Michael Kadar-Kallen, Lou Castagna
Tyco Electronics
PO Box 3608, Harrisburg, PA 17105
email: mgurreri@tycoelectronics.com

Darrell Childers, Mike Hughes
US Conec, Ltd.
1555 4th Avenue SE, Hickory, NC 28602
email: mikehughes@USConec.com

Abstract: This paper describes a simplified model linking MT ferrule and connector attributes to positive contact performance. Validation with FEA, experimental apparatus and empirical results are described, along with topics for future study.

OCIS codes: (060.2340) Fiber Optics Components; (120.3180) Interferometry

1. Introduction

Multi-fiber, monolithic MT ferrules are used in a wide variety of optical interconnect applications including bulkhead feed-through connectivity, optical backplanes and outside plant passive optical networks. The typical MT ferrule is comprised of at least one fiber array with up to twelve 125μm diameter fibers on 250μm centerline spacing. The MT ferrule has a rectangular cross-section of 2.4mm X 6.4mm and a depth of 8mm. The ferrules are generally molded from a highly glass-filled, thermoplastic or thermoset resin, which combines the durability and stability required of a connector with the precision necessary to maintain low-loss singlemode core-to-core alignment across multiple fibers. Although single row ferrules with four, eight or twelve fibers are the most common, multi-row MT ferrules with up to 72 fibers are now readily available. This high density interconnect package offers a compact, convenient means for quickly and effectively distributing large numbers of fibers.

To assure precision alignment between two mating MT ferrule based connectors, a non-interference, dual guide pin and hole system is used. One connector in the pair typically houses both guide pins while the mating, unpinned connector ferrule receives the guide pins when mated. The pinned and unpinned ferrules have identical geometry.

In order to establish a reliable, dry, low insertion loss and low reflectance junction, physical contact between each fiber tip is imperative. Even with very accurate core-to-core alignment, power loss from Fresnel effects, which are associated with gaps between fiber tips, will not meet the requirements of today's WDM and Passive Optical Network applications. To achieve physical contact, the ferrule endface is prepared such that the fiber tips are protruding from the ferrule surface.

Optical transmission systems have historically employed physical contact connectors that are based on single-fiber cylindrical ferrules. To establish dimensional limits on the end face geometry, such that physical contact is maintained, the mechanics of single-fiber connectors have been studied extensively [1,2]. These studies employed finite element analysis (FEA), boundary element methods, Hertzian analysis, and experimentation to develop a comprehensive understanding of the interface under various environmental and mechanical conditions [3-7]. Given that MT connectors have emerged as a de facto standard for high density applications, similar evaluations will allow for meaningful specification of the governing end face variables.

The two primary parameters, which impact the ability to obtain physical contact in an MT connector system are (1) the coplanarity of the protruded fiber tip and (2) the angular accuracy in both axes of the ferrule endface relative to the guide pin bores. Even the most advanced and well-controlled mass production processes today produce fiber arrays with some variation in fiber tip protrusion and angular endface accuracy. Any imprecision of this nature must be overcome by deformation due to the connector spring mechanism to obtain physical contact of mating fiber tips. Gaps between the fiber tips resulting from these manufacturing inaccuracies are illustrated in Figure 1.

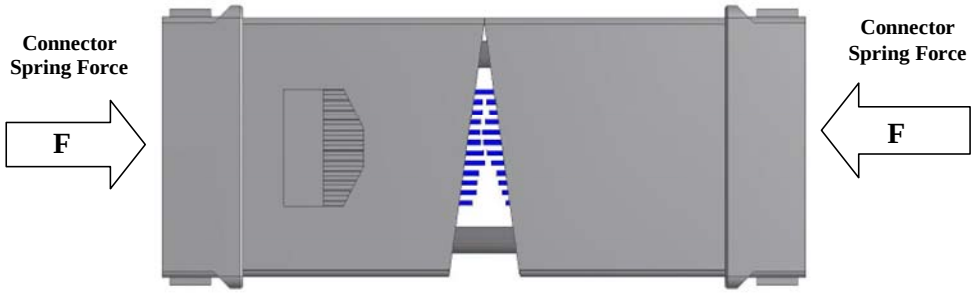

Figure 1: Schematic of MT ferrule pair with exaggerated manufacturing inaccuracies to be overcome by the connector spring mechanism

Two primary ferrule attributes that determine the connector endface geometry requirements for physical contact are the fiber tip stiffness and rotational stiffness. The focus of this research is on the fiber tip stiffness. The fiber tip stiffness will dictate the industry specification for fiber tip coplanarity [8] across an array of fibers. Coplanarity is the difference between the maximum and minimum fiber tip protrusions relative to a best-fit line through the fiber tip array distribution.

2. Theory

A three-stage analytical approach was taken to examine the force required to displace the tip of a single fiber in an MT ferrule when an axial load is applied to the fiber. First, a full three-dimensional finite element model was created as a baseline. Then, for computational efficiency, a two-dimensional axisymmetric finite element model was created to explore a variety of fiber tip radii to determine a composite "fiber stiffness" that includes the elasticity of the ferrule, fiber and epoxy regions. This stiffness became the basis of an even more simplified model wherein each fiber is represented by a spring. The behavior was verified experimentally by mating specially prepared samples against a transparent rigid plate and using interferometry to observe fiber contact.

2.1. Three dimensional FEA

The three-dimensional FEA was performed on a single row, 12-fiber MT ferrule to observe the deflection with a single load applied to the fiber under study. The model, which included material properties for the ferrule, fibers, and bonding epoxy, was constrained at the base of the ferrule and subjected to a 1N distributed load on one of the central fibers. The compressive deflection results of the model are illustrated in Figure 2. It was observed that the displacement field is radially symmetric in the region of interest. This finding indicates that a two-dimensional, axis-symmetric model can be used to simplify the analysis. There are also larger, asymmetric displacement contours, due to the presence of an epoxy window on one side of the ferrule. However, this deflection, which is relatively low in magnitude, had an inconsequential effect on the overall system stiffness.

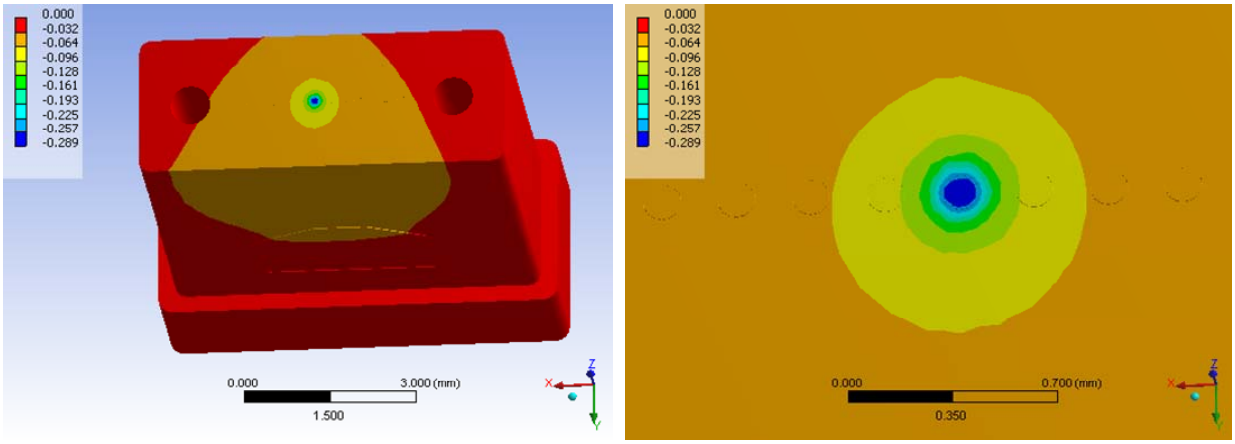

Figure 2: 3D FEA model with load applied to one center fiber. The color gradient represents the Z-axis deflection field.

In addition, it was determined that a foundation effect is present such that, when displacing a single fiber, the stress zone within the ferrule body is large enough to influence the fiber tip location of adjacent fibers. Notable adjacent fiber displacement was detected at fiber locations 250μm, 500μm, and 750μm away from the fiber under load. This discovery suggests that the displacement of each fiber tip is related not only to the reaction force of that particular fiber, but also to the applied forces on neighboring fibers. These discoveries led to a conceptual model that includes an elastic base as shown in Figure 3.

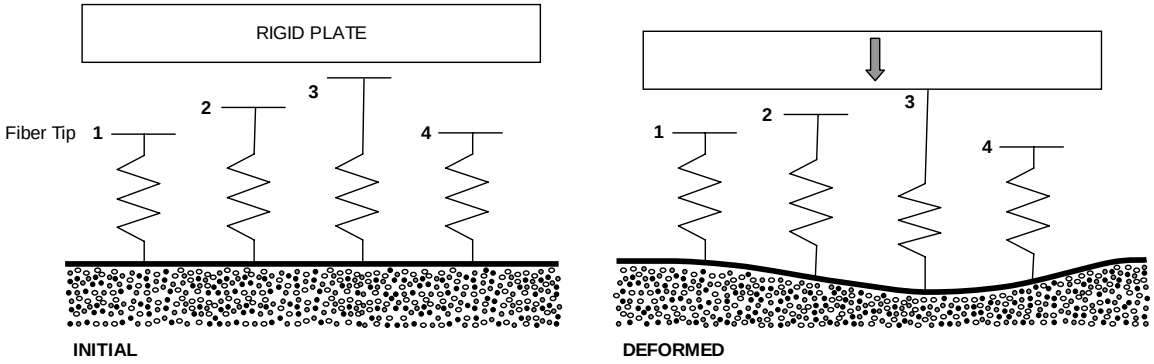

Figure 3: Simplified conceptual model of four fiber MT ferrule fiber tips compressed by a rigid plate showing the foundation effect.

2.2. Two dimensional axisymmetric FEA

Based on evaluation of the complete, three-dimensional model results, an axisymmetric FEA was generated. This yielded a streamlined approach that allowed parametric adjustment of the dominant variables, including the geometry, material properties, and load conditions. As shown in Figure 4, a cross-sectional slice was taken through one of the individual fiber centers. This cross-section included regions for the optical fiber, epoxy layer, and ferrule, and the material properties were based on published literature values. The boundary conditions included a fixed displacement to a rigid plate, which contacts a spherically shaped fiber tip, and fixed constraints on the ferrule exterior. Other pertinent details of the model are defined in Appendix A.

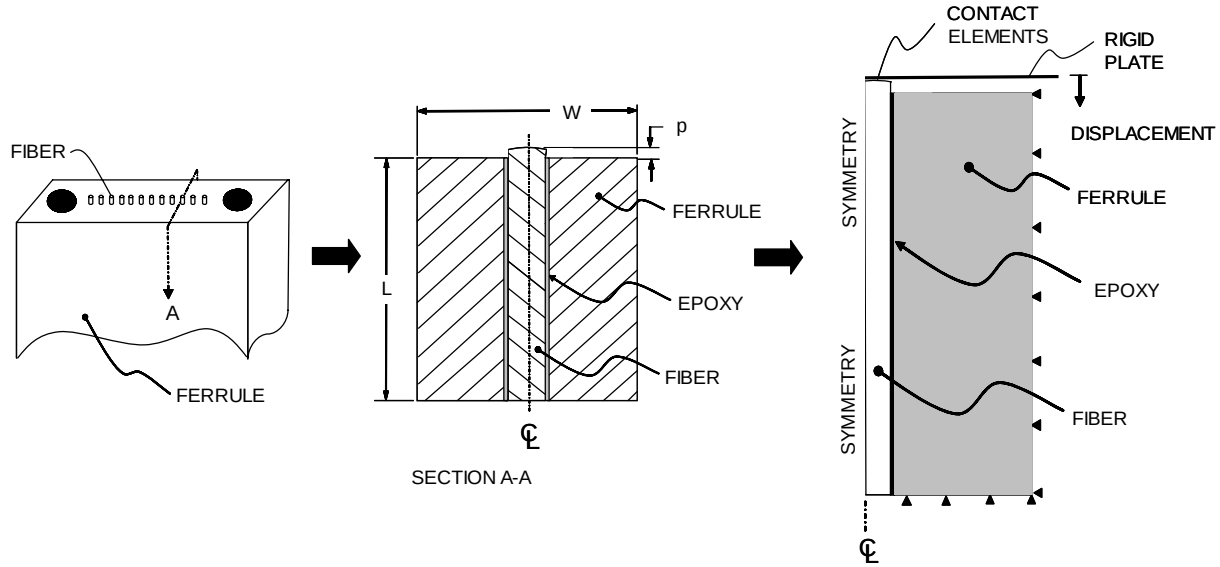

Figure 4: 2D Axisymmetric Model Concept with load applied to one fiber.

To validate this two-dimensional model, the fiber reaction force and displacements were compared to the more computationally intense, three-dimensional analysis. It was found that the two models produced nearly identical results for the fiber under load, as well as the neighboring unloaded fibers at 250μm, 500μm and 750μm. The

contour plot shown in Figure 5 illustrates the axial deflection of the system given a 2μm displacement of the rigid plate. This demonstrates that a significant portion of the system elasticity is attributable to compression of the ferrule region due to the relatively large displacement zone.

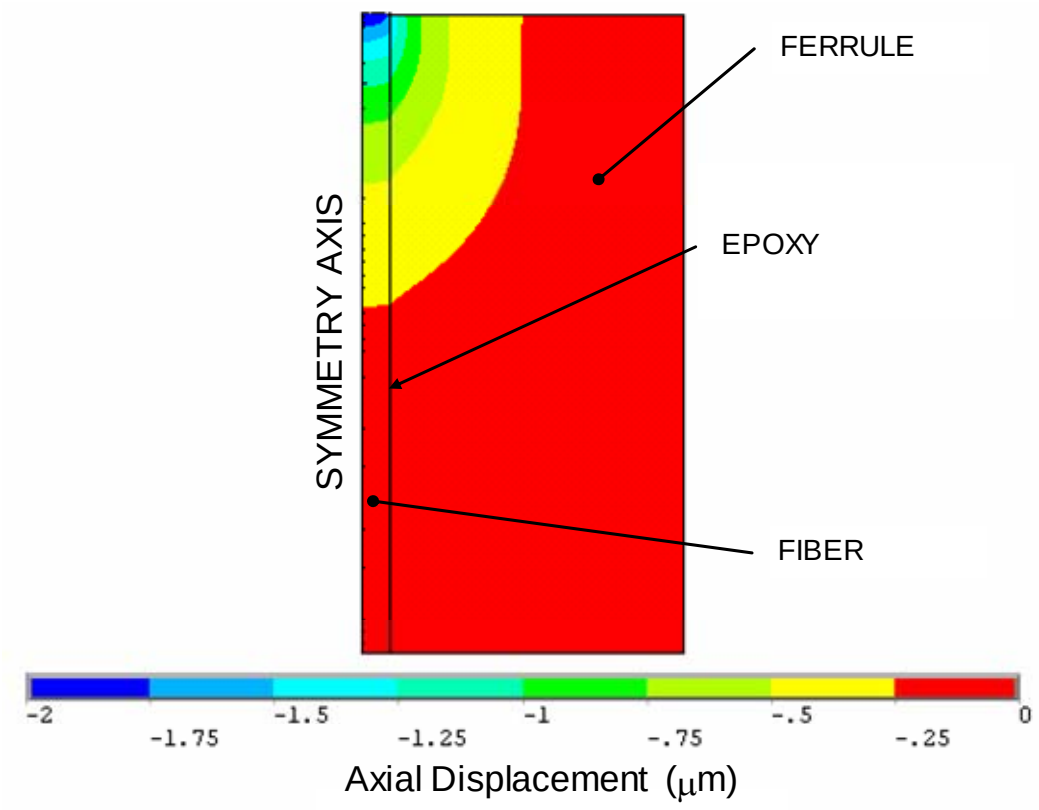

Figure 5: Axial deflection results for a 2μm displacement of the fiber tip

Several iterations of the model were run with various fiber tip profiles and loads to understand how these parameters influence the overall system stiffness. To summarize the results, Figure 6 shows a graph of the fiber reaction forces, which are plotted as a function of tip displacement, for a family of different radius cases. This data reveals several critical traits of the overall system behavior. As the fiber tip radius decreases, the equivalent spring constant, as illustrated by the slope of the curves, is significantly reduced. The case with the highest stiffness, which is associated with a flat fiber tip (infinite radius), has a spring rate of about 4.2 N/μm while the 1mm case has a rate of about 2.1 N/μm. Furthermore, as the fiber tip radius decreases, the linearity of the spring constant diminishes. This suggests that there are two components to the fiber tip displacement: (1) The composite stiffness of the ferrule, fiber, and epoxy, and (2) the classical Hertzian contact deformation of the glass fiber tip. For large fiber tip radii, the composite stiffness is largely responsible for tip displacement, while the Hertzian effect plays a minor role; whereas, for small radii, the impact of the Hertzian component becomes noticeable.

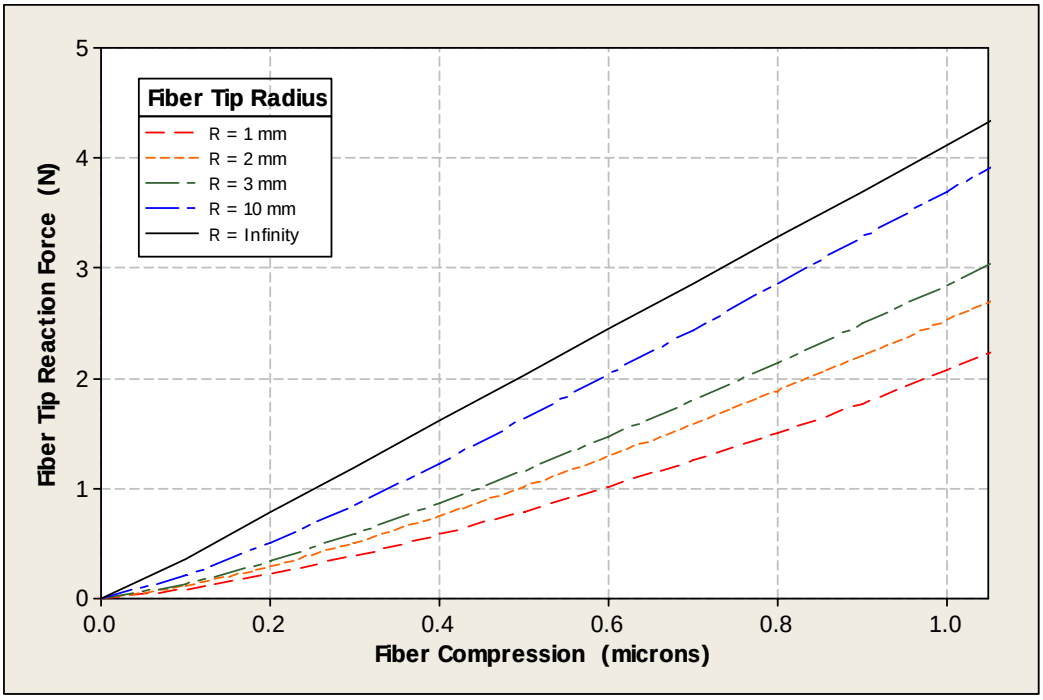

Figure 6: Fiber tip reaction force as a function of compression and fiber tip radius. Note the nonlinear behavior increases as the tip radius decreases.

Figure 7 demonstrates the foundational effect: the displacement of fibers other than the fiber to which the force is applied, caused by the deformation of the MT ferrule "foundation". The displacements of the other fibers are linear functions of the applied force, independent of the radius of the tip of the fiber to which the force is applied.

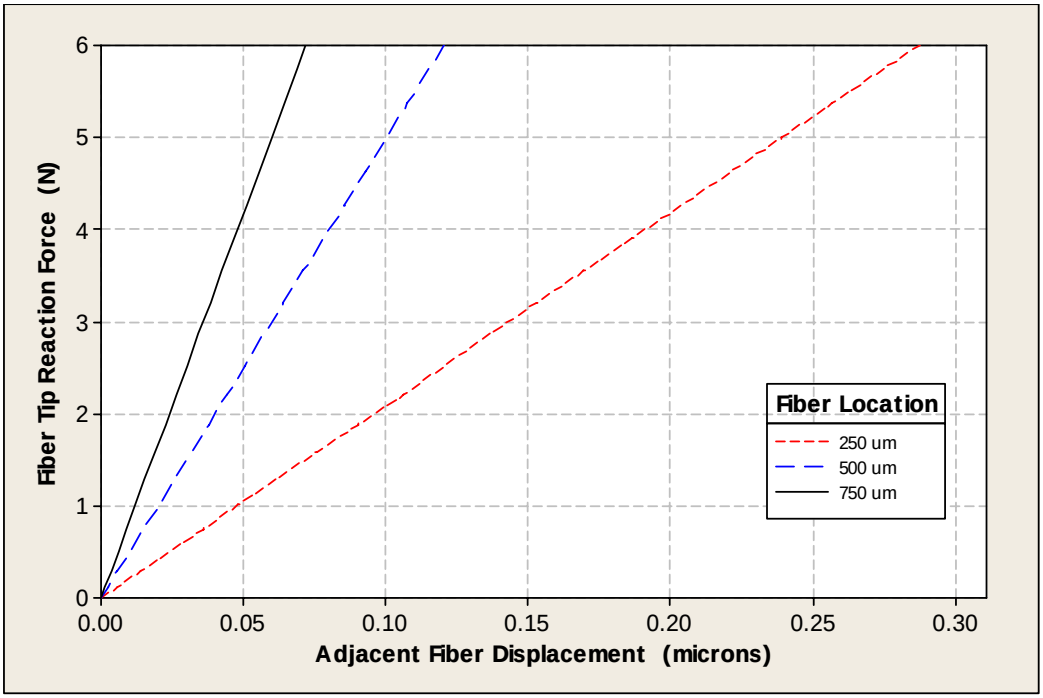

Figure 7: Fiber tip reaction force as a function of adjacent fiber displacement.

3. Simplified Mathematical Model

A simplified mathematical model based on the fiber tip displacement vs. force FEA analysis was developed to quickly and accurately predict the forces required for physical contact for actual ferrule geometries. Figure 8 defines the parameters that were used to generate this model.

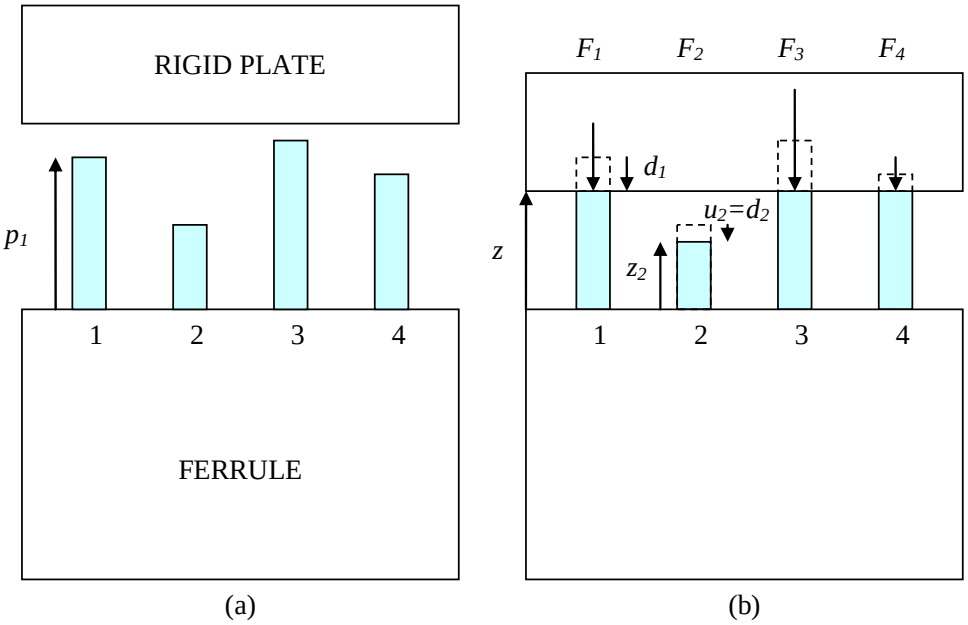

Figure 8: Model Parameters: (a) Fiber protrusion in the absence of an applied force; (b) A rigid plate is at a distance z such that some fibers are in contact with the plate.

The displacement of an individual fiber tip d_i is the difference between the initial protrusion p_i and the protrusion z_i under an applied load:

$$d_i = p_i - z_i . \tag{1}$$

Note that z_i is measured with respect to the initial, undeformed ferrule surface. This displacement consists of two components:

$$d_i = \Delta_i + u_i , \tag{2}$$

where Δ_i is the compression of the fiber i due to the force F_i applied to fiber i and u_i is the displacement of the foundation of fiber i due to the forces applied to the other fibers.

From Figure 7 it can be seen that the displacement of the foundation of fiber i due to the forces applied to the other fibers is a linear function. The displacement of the foundation of fiber i can therefore be modeled as a series of springs such that:

$$u_i = \sum_{j<>i} \frac{F_j}{k_{ij}} \quad , \tag{3}$$

where k_{ij} is the spring constant which couples fiber i and fiber j.

By combining Equations 1, 2, and 3, the following equation for the fiber tip protrusion under load is derived:

$$z_i = p_i - \Delta_i - \sum_{j<>i} \frac{F_j}{k_{ij}} . \tag{4}$$

The force F_i applied to a fiber tip is related to the compression Δ_i caused by this force and to the radius of curvature r_i of the fiber, as shown in Figure 6. Note that $\Delta_i = 0$ if and only if $F_i = 0$.

Applying the following boundary conditions for a given rigid plane at a distance z from the ferrule defines a set of N simultaneous equations with N unknowns: the forces F_i, or the corresponding compressions Δ_i

$$z_i = z \text{ if } z < p_i - u_i$$

$$z_i = p_i - u_i \text{ if } z \geq p_i - u_i \,. \tag{5}$$

By varying the value of z and solving the set of equations for each value of F_i , the minimum force required to achieve contact with the rigid plate can be determined. The total force applied to the rigid plate is simply

$$F = \sum F_i \,. \tag{6}$$

4. Experimental Methodology

To assess the validity of the theoretical models, MT ferrule assemblies were created with end face geometries designed specifically to facilitate the experiment. This was accomplished by polishing such that the fiber tip elevations lay along a curved profile with varying deviation (coplanarity). These parts were characterized interferometrically for coplanarity of the fiber tips as well as for shape of the individual fibers. A sample fiber tip radius is shown in Figure 9.

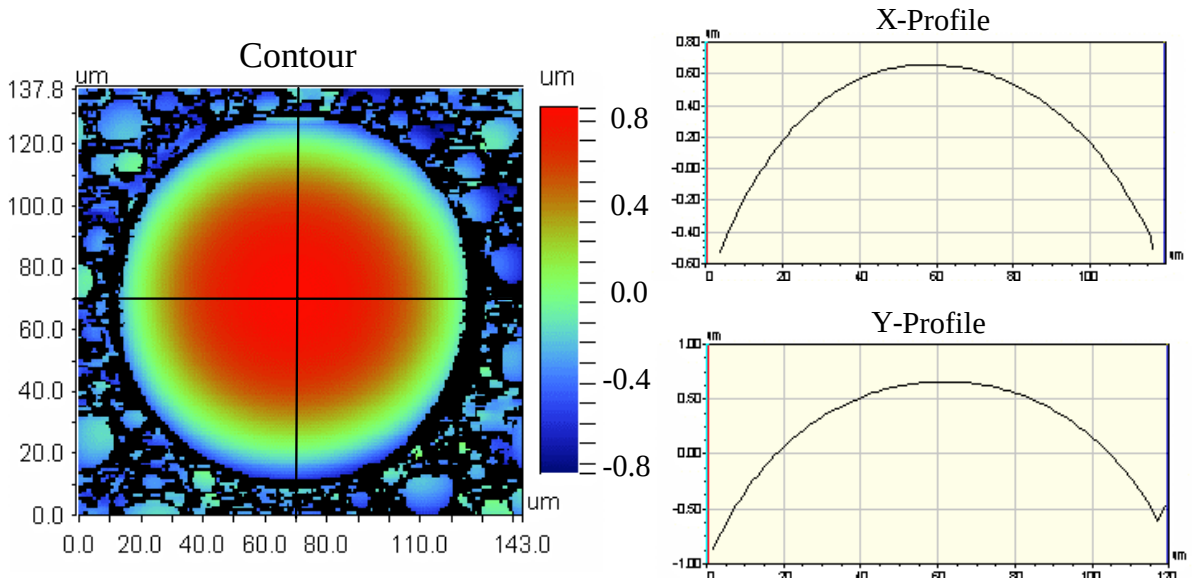

Figure 9: Typical interferometric endface analysis of fiber tip

An experiment was then set up to evaluate the forces required to bring the various protruded fiber tip heights into contact with a transparent rigid body. By shining white light through the transparent body onto the ferrule endface, fiber tip contact with the body can be observed through a microscope when the reflection of light traveling through the body onto the polished fiber tips is eliminated by physical contact. At the point of fiber contact with the transparent rigid body, light is no longer reflected from the fiber tips, but rather transmitted into the fiber resulting in a dark contact region on the fiber tip.

The transparent rigid body is mounted onto a stage with precision angular alignment control in both primary axes. The angular alignment control of the rigid body provides a means to ensure physical contact with only the protruded fiber tips. The MT ferrule is mounted to a load cell for capturing the forces transmitted by the rigid body for various stages of fiber tip physical contact. By documenting the amount of force required to bring known fiber tip heights into contact with the optical flat, the theoretical deflection vs. reaction force model can be compared with actual empirical data. A schematic of the experimental apparatus is illustrated in Figure 10.

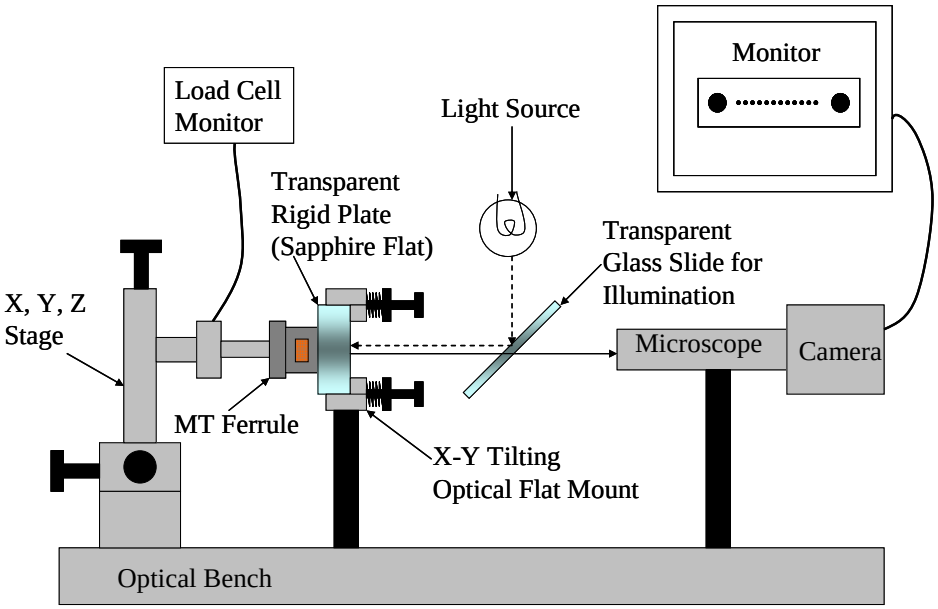

Figure 10: Apparatus for measuring fiber tip deflection vs. reaction force

The polishing process used for the experimental MT ferrules yielded a fiber tip distribution such that the fiber tips in the center of the array protruded the most, while the fiber tips on the ends of the protruded the least. As a result, the outermost fiber tips are the last to come into contact when force is applied with a flat, rigid body. An example of the Tip Deflection vs. Reaction Force data collected for a typical MT endface is shown in Figure 11.

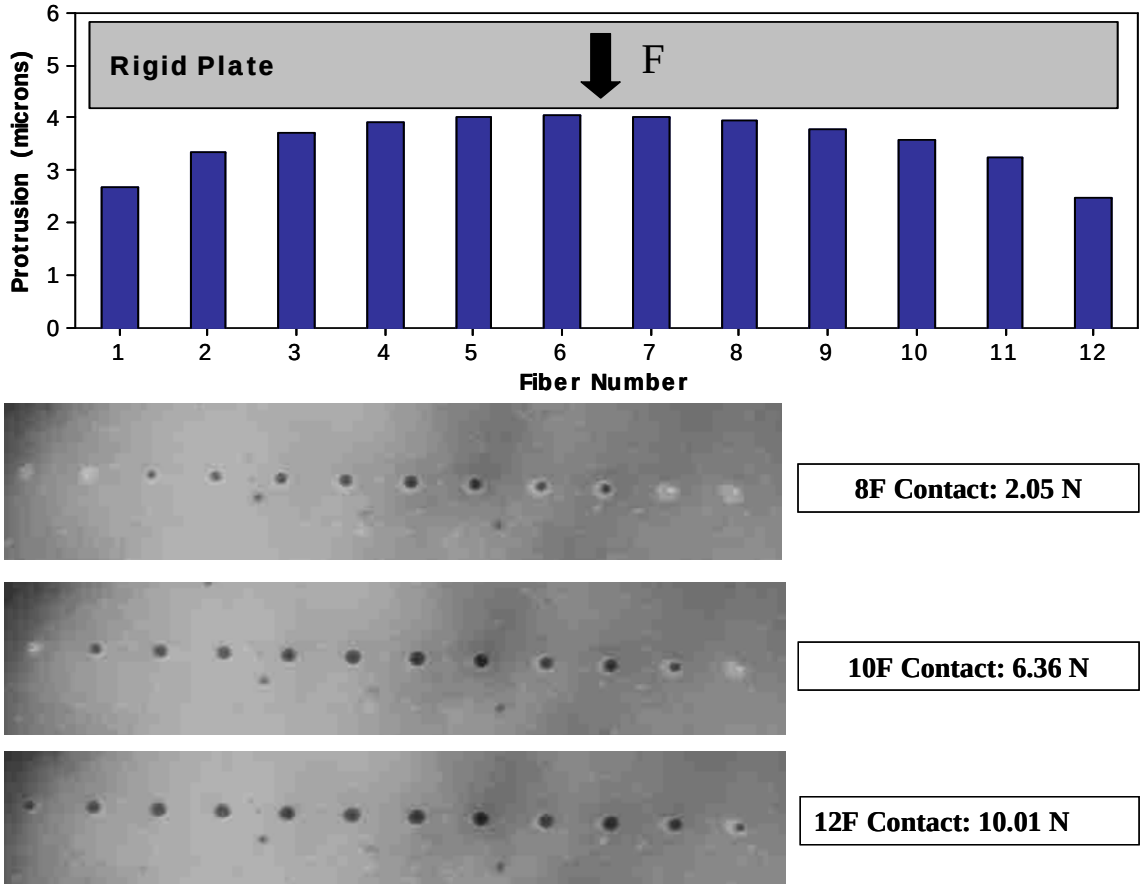

Figure 11: Sample tip deflection vs. reaction force data

5. Empirical and Theoretical Results

The force required to bring fiber tips into contact with the rigid plate was compared to the theoretical force as calculated by the simplified mathematical model. Ferrules characterized with sharp fiber tip radii (1-2mm) and flat fiber tips (>10mm) were analyzed. Figure 12 illustrates a comparison of theoretical and empirical results for ferrules that had polished fiber tip radii ranging between 1mm and 2mm.

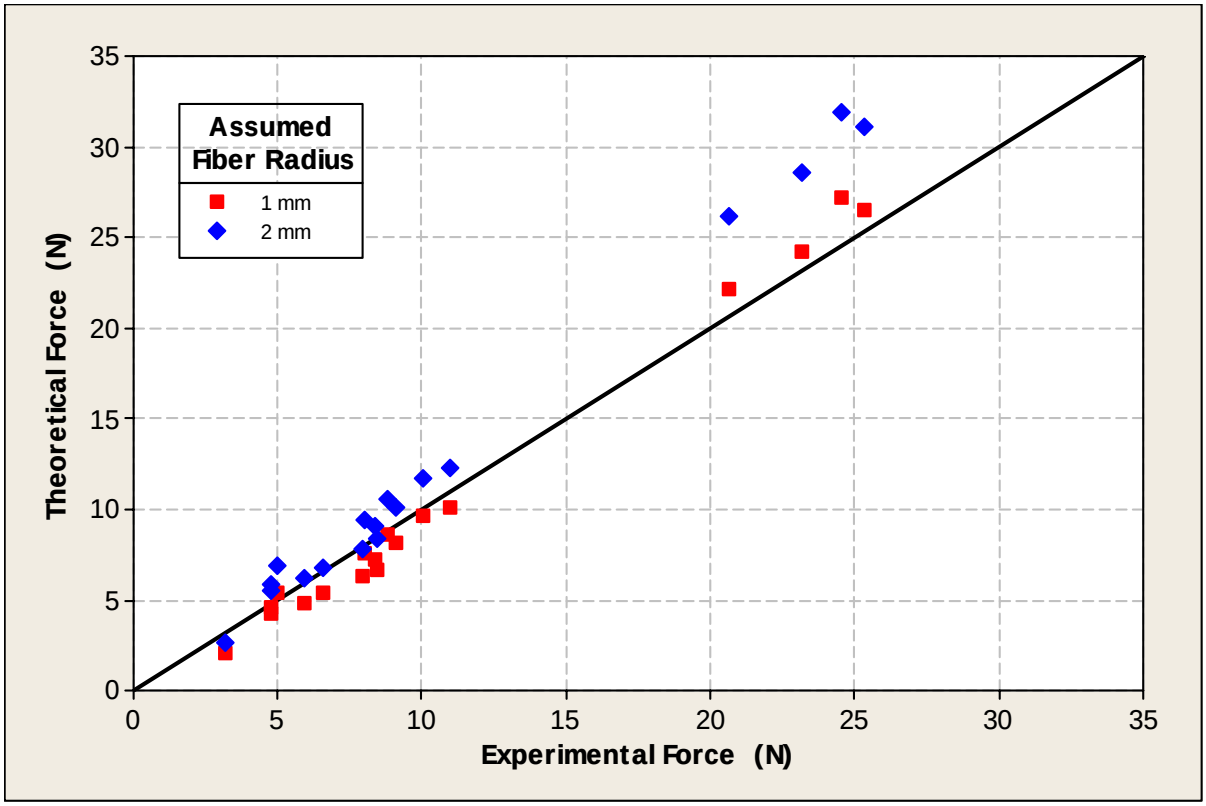

Figure 12: A comparison of the experimental and theoretical results. For each experimental data force value, two theoretical points are plotted, corresponding to 1 mm and 2 mm fiber radii of curvature.

To investigate system repeatability in addition to presence of any inelastic behavior, a set of previously unmated ferrules was measured for physical contact force over repeated compression cycles. Ten repeated iterations of compressing the fiber tips onto the rigid plate for various fiber tip coplanarities were followed by 50 MPO mating cycles. A final fiber tip compression experiment was performed. The forces required to bring all fibers into contact are shown in Figure 13 and suggest no hysteresis effect from repeated MT connector mating cycles.

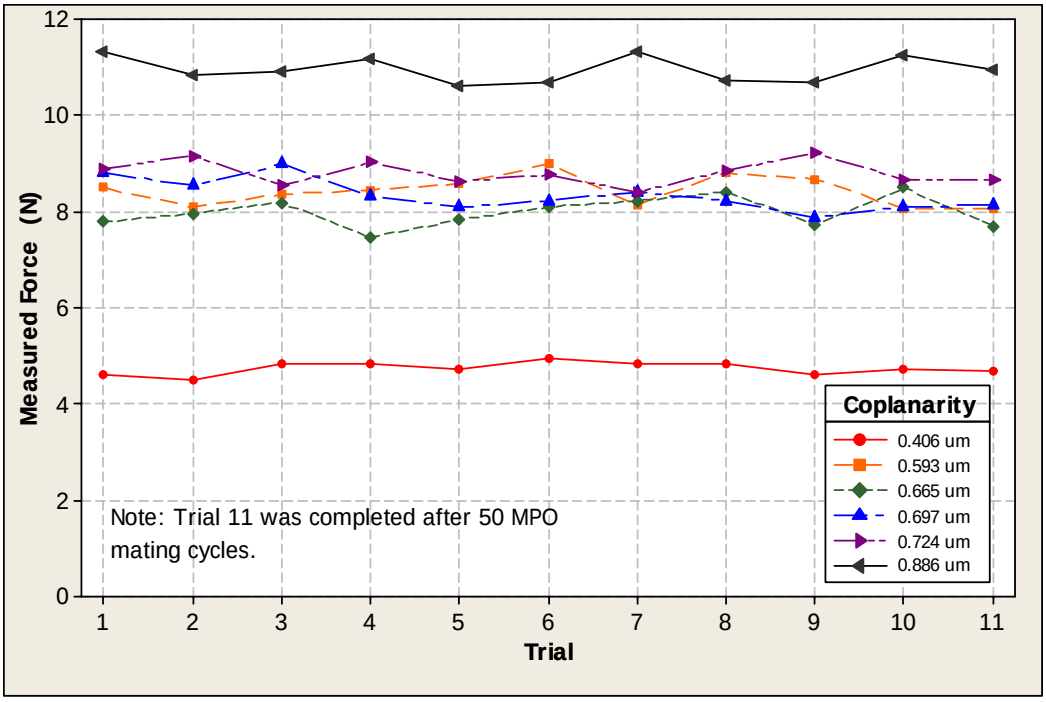

Figure 13: Compression force required for physical contact over repeated cycles. 50 MPO cycles were performed on the samples between trials 10 and 11.

The amount of force required to bring fiber tips into contact with a rigid plate is directly related to the degree to which the fiber tip elevations deviate from a single plane. Typical polishing processes will yield a distribution of fiber tip elevations that closely follows the ferrule surface profile. Figure 14 shows the circular shape of MT ferrule fiber tip distributions created for this experiment.

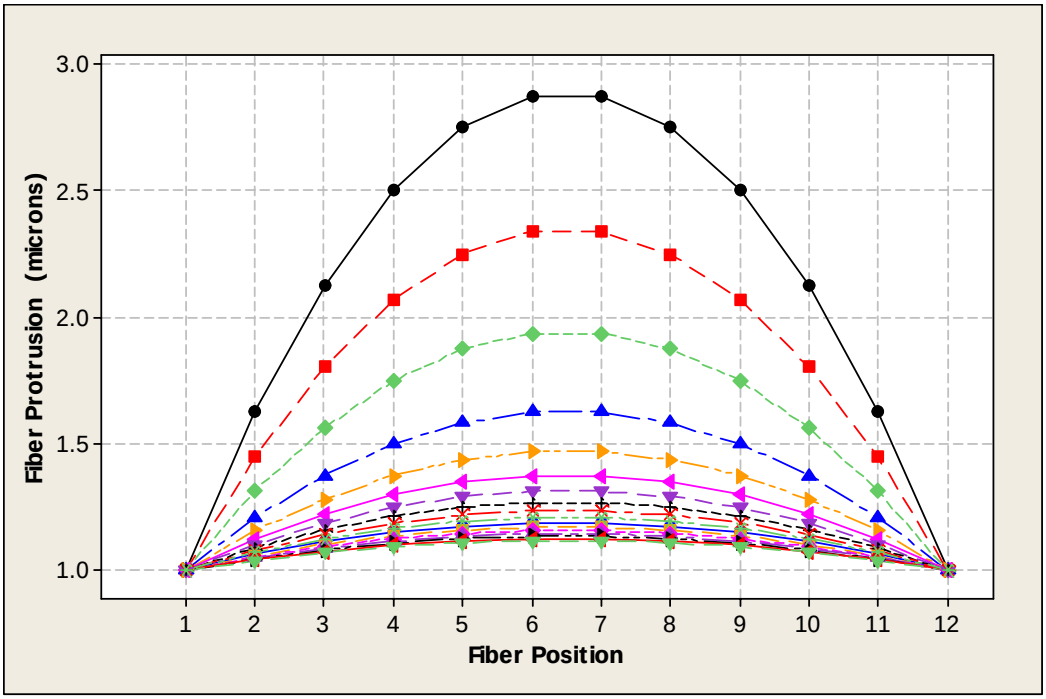

Figure 14: Exaggerated curved shape for MT fiber tip height distribution. Each curve is in fact a circular arc.

By assuming fiber tip elevations are distributed in a circular shape, the theoretical force required for physical contact can be approximated as a function of fiber tip coplanarity. A Force Vs. Coplanarity curve is illustrated in Figure 15 for flat (10mm – Infinite) and radiused (1mm-2mm) fiber tips. Experimental results for both flat and radiused fiber tips are plotted along the theoretical curves. Given the degree of experimental uncertainty and sample variability, the correlation between the theory and experiment shows excellent agreement.

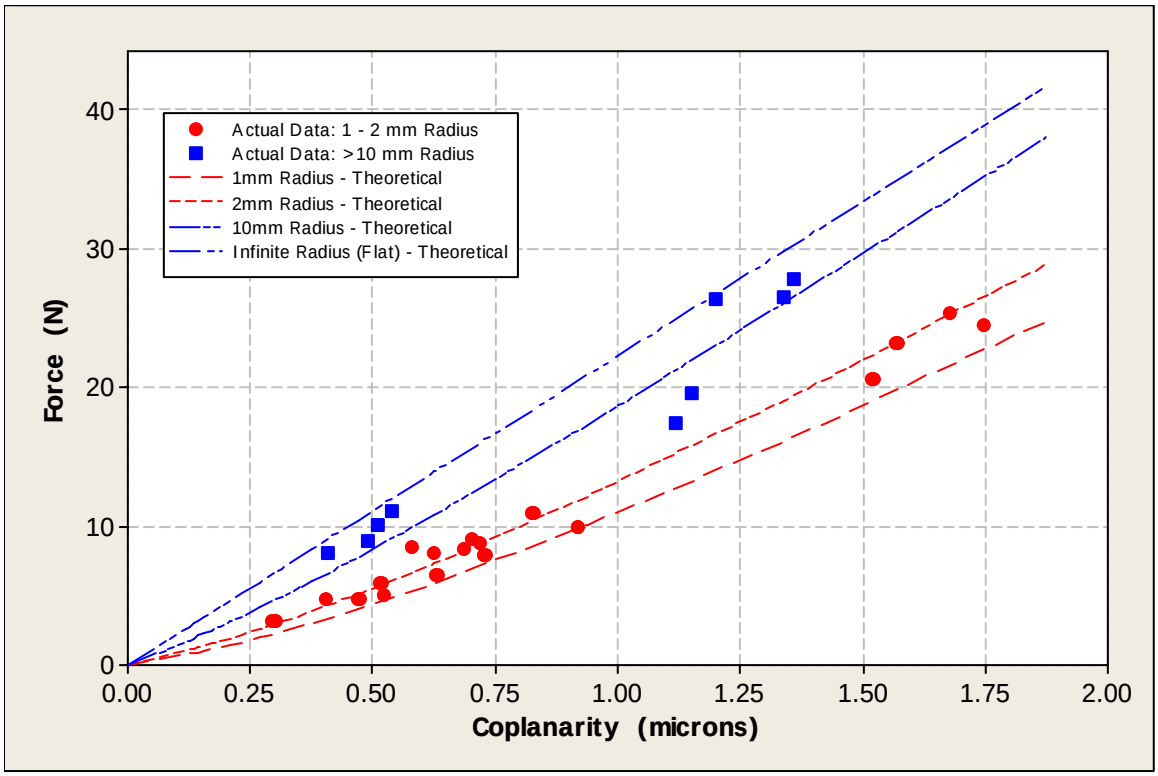

Figure 15: Force required for physical contact as a function of coplanarity for 1-2mm radius and >10mm fiber tips. Theoretical fiber tip distributions are radiused in shape as illustrated in Figure 14

6. Conclusions

A theoretical model to simulate MT fiber tip compression has been generated and verified empirically. This model will be used as a foundation to further develop MT endface geometry requirements.

The amount of compression force required to bring differing MT fiber tip heights into contact is highly dependent on ferrule material modulus. The ferrule material foundation deflection due to loads applied to a single fiber will also result in relative deflection of adjacent fiber tips. This foundation effect requires a complex analysis of the interaction between all fiber tip reaction forces within a single ferrule to predict forces required for physical contact.

Due to a classical Hertzian deformation component of the fiber tip deflection, the fiber tip shape is a key MT endface geometry parameter to be considered when formulating intermateability standards. Depending on the coplanarity, ferrules polished with perfectly flat shaped fiber tips can require as much as 80% more force for physical contact as ferrules polished with 2mm radius fiber tips.

7. Future Work

Fiber tip stiffness is but one attribute which impacts the geometric optical interface specifications required to establish key MT ferrule connector physical contact. Angular mismatch and rotation stiffness in both X and Y axes must also be thoroughly characterized to complete a room temperature physical contact model for MT ferrules. The impact of operating environment on these parameters must also be studied to determine endface geometry specifications for specific applications.

8. Acknowledgements

Eric Childers and Dr. Toshiaki Satake: Empirical experiment development
Ton Bolhaar and Robert Peters: Fiber tip radius measurement.
Mark Thompson: Endface geometry interferometer measurements.

9. References

[1] Nagase, R., Shintaku, T., Sugita, E., "Effect of Axial Compressive Force for Connection Stability in PC Optical Fibre Connectors", IEEE Electronics Letters, Trans. Photonic Tech. Lett., Vol. 23, No. 3, pp. 103 – 105, (1987).
[2] Shintaku, T., Nagase, R., Sugita, E., "Connection Mechanism of Physical-Contact Optical Fiber Connectors with Spherical Convex Polished Ends", Applied Optics, Vol. 30, No. 36, pp. 5260 – 5265, (Optical Society of America 1991).
[3] Deeg, E. W., "Effect of Elastic Properties of Ferrule Materials on Fiber-Optic Physical Contact (PC) Connection", AMP Journal of Technology, Vol. 1: 25-31, (1991).
[4] Deeg, E. W., "New Algorithms for Calculating Hertizian Stresses, Deformations, and Contact Zone Parameters", AMP Journal of Technology, Vol. 2, pp. 14-24, (1992).
[5] Reith, L. A., Grimado, P. B., and Brickel, "Effect of Ferrule-Endface Geometry on Connector Intermateability", in Technical Proceedings, NFOEC 1995, Vol. 4, (1995).
[6] Breedis, J. B., and Manning, R. M., "Simulating the End-Face Deformation of Physical Contact (PC) Optical Connectors", AMP Research Report, (1997).
[7] Bolhaar, T., "PC Connector Interface Parameters for Datacom Detail Specifications", IEC 86B (Ottawa 1996).
[8] Knecht, D., Luther, J., Pyatt, J., and Ugolini, A., "Recent Advances in MT Ferrule Processing and MTP Hardware Design", in Technical Proceedings, OFC, (Optical Society of America, 2005)

Appendix A – FEA Model Material and Geometric Properties

The finite element models were generated using properties for a glass-filled polyphenylene sulphide (PPS) ferrule material. Specific values of the elastic modulus, E, and Poisson's ratio, ν, are defined in Table A.1 for the ferrule, fiber, and epoxy regions. The materials were assumed to behave in a linear elastic manner.

Table A.1: Material properties used in finite element analysis

Material	**E** (MPa)	ν
Fiber	73000	0.17
Ferrule	18000	0.35
Epoxy	5000	0.40

The model was constructed with a nominal fiber diameter of 125μm and an annular epoxy layer thickness of 0.5μm. The fiber, epoxy, and ferrule regions were bonded such that no shear slippage could occur at the boundaries. In addition, to validate the experimental setup, there was a previous analysis that included material properties for a sapphire optical flat. However, it was found that this flat could be treated as infinitely rigid since the modulus, which is approximately 345 GPa, was several times larger than the other component moduli.